Tritium NMR Spectroscopy of Ligand Binding to Maltose-Binding Protein†

Kalle Gehring,‡,§ Philip G. Williams,‖ Jeffrey G. Pelton,‡ Hiromi Morimoto,‖ and David E. Wemmer*,‡

Chemical Biodynamics and National Tritium Labeling Facility, Lawrence Berkeley Laboratory, University of California, Berkeley, California 94720

Received November 27, 1990; Revised Manuscript Received February 27, 1991

ABSTRACT: Tritium-labeled α- and β-maltodextrins have been used to study their complexes with maltose-binding protein (MBP), a 40-kDa bacterial protein. Five substrates, from maltose to maltohexaose, were labeled at their reducing ends and their binding studied. Tritium NMR spectroscopy of the labeled sugars showed large upfield chemical shift changes upon binding and strong anomeric specificity. At 10 °C, MBP bound α-maltose with 2.7 ± 0.5-fold higher affinity than β-maltose, and, for longer maltodextrins, the ratio of affinities (K_D^{β}/K_D^{α}) was even larger (between 10 and 30). The maximum chemical shift change was 2.2 ppm, suggesting that the reducing end of bound α-maltodextrin makes close contact with an aromatic residue in the MBP-binding site. Experiments with maltotriose (and longer maltodextrins) also revealed the presence of two bound β-maltotriose resonances in rapid exchange. We interpret these two resonances as arising from two distinct sugar–protein complexes. In one complex, the β-maltodextrin is bound by its reducing end, and, in the other complex, the β-maltodextrin is bound by the middle glucose residue(s). This interpretation also suggests how MBP is able to bind both linear and circular maltodextrins.

Maltose-binding protein (MBP)[1] is a soluble, monomeric periplasmic protein from *Escherichia coli* involved in the transport of maltodextrins across the cytoplasmic membrane and in chemotaxis toward maltodextrins (Schwartz, 1987). In vitro, MBP binds linear and circular maltodextrin molecules [α(1–4)-linked D-glucose polymers] with high affinity (K_D = ~1 μM) and a stoichiometry of one ligand per MBP molecule (Kellerman & Ferenci, 1982). The preliminary X-ray crystal structure of MBP shows two folded domains connected by a hinge region in strong similarity to other periplasmic binding proteins (Spurlino, 1988; Adams & Oxender, 1989). By analogy to other binding proteins, it is believed that the two domains come together and clamp down on the substrate during binding (Mao et al., 1982). Conformational changes in MBP and other binding proteins during substrate binding have been observed by fluorescence energy transfer (Zukin, 1979), small-angle neutron scattering (Newcomer et al., 1981), fluorescence spectroscopy (Szmlecman et al., 1976; Miller et al., 1983), optical spectroscopy (Trakhanov et al., 1989), and proton and fluorine NMR spectroscopy (Clark et al., 1982; Shen et al., 1989a,b; Post et al., 1984; Chauvet-Monges et al., 1979).

Anomeric specificity in sugar-binding proteins has generally been a difficult subject to study because of the interconversion between sugar anomers in solution. This is particularly true for maltose and maltodextrins where only the β anomer is readily available in crystalline form (Greenwood, 1970; Hodge et al., 1972; Takusagawa & Jacobson, 1978). Among periplasmic binding proteins, only in the case of arabinose-binding protein, which has been crystallized with a mixture of α- and β-arabinose, is the degree of anomeric specificity known with any precision [Miller et al., 1983; Quiocho & Vyas, 1984; reviewed in Quiocho (1986)]. NMR spectroscopy, because of its high sensitivity to molecular conformations, is a good technique for studying anomeric specificity. For example, studies of *N*-acetylglucosamine (NAG) binding to lysozyme detected a splitting of the NAG methyl resonances due to differences in affinity of the two anomeric forms of NAG (Sykes, 1969; Raftery et al., 1968; Thomas, 1966). These studies, however, were limited to studying processes in the fast-exchange limit where a large excess of substrate could be used.

Tritium NMR spectroscopy with its high relative sensitivity and selectivity extends the capability of NMR spectroscopy for studying anomeric specificity to slowly exchanging processes at low stoichiometries of ligand to binding sites. We have previously used tritium-labeled maltose to study its binding to MBP (Williams et al., 1989). Unlike arabinose-binding protein, MBP shows anomeric specificity and binds α-maltose with 2- to 3-fold higher affinity than β-maltose. In the present study, we have expanded our study to the family of linear maltodextrins (of which maltose is the smallest member). This has revealed stronger anomeric specificity with longer maltodextrins and two modes of maltodextrin binding to MBP: one mode with the reducing end of the oligosaccharide in the protein binding site and the second mode with the middle of the oligosaccharide in the protein binding site. The balance between these two binding modes is influenced by the length of the oligosaccharide and by the anomeric conformation of the reducing end. The binding of circular maltodextrins to MBP occurs by the second mode with an

† This work was supported by National Institutes of Health Grant P41 RR01237 to the NTLF. K.G. was supported by a DOE Alexander Hollaender postdoctoral fellowship. General support was provided by the Office of Energy Research, Health Effects Research Division, of the U.S. Department of Energy (Contract DE-AC03-76SF0098) and equipment grants from DOE, DE-FG05-86ER75281, and NSF, DMB 86-09035.

* Author to whom correspondence should be addressed.

‡ Chemical Biodynamics.

§ Present address: Group de Biophysique, Ecole Polytechnique, 91128 Palaiseau, France.

‖ National Tritium Labeling Facility.

[1] Abbreviations: NMR, nuclear magnetic resonance; MBP, maltose-binding protein; G2, maltose; G3, maltotriose; G4, maltotetraose; G5, maltopentaose; G6, maltohexaose; [1-^{3}H]maltotriose, [D-glucopyranose-α(1–4)]$_2$-D-[1-^{3}H]glucopyranose; 2-D, two dimensional; EXSY, 2-D chemical-exchange spectroscopy; TPPI, time-proportional phase increment; NAG, 2-acetamido-2-deoxy-D-glucose; triton, ^{3}H nucleus.

0006-2960/91/0430-5524$02.50/0

affinity consistent with that observed for linear maltodextrins binding in the same mode.

Materials and Methods

Tritium Labeling. Maltodextrins, linear α(1–4)glucopyranose polymers ranging from maltose (G2; two glucose residues) to maltohexaose (G6; six glucose residues), were labeled by exchange with tritium gas in the presence of palladium (5%) on $BaSO_4$ (Evans et al., 1974). Specifically, 0.5 mL of 0.24 M sugar solution in 0.1 M Na·HPO_4, pH 7, was degassed and 20 mL of carrier-free tritium gas at 1 atm added to the reaction vessel. The reduced palladium catalyst was then added to the solution and the mixture stirred at ambient temperature. After 2 h, the tritium gas was removed, the catalyst was removed by filtration, and the sample was lyophilized to remove labeled water ($^3H^1HO$). The activity of the labeled sugars was measured by liquid scintillation counting, and the specific activities were estimated by assuming complete recovery of sugar from the labeling reaction. Maltodextrins labeled in this way had specific activities of 2.5–10 Ci/mmol (8–33% label at the C1 position). Tritium labeling of maltodextrins was performed at the National Tritium Labeling Facility, which is equipped with the necessary vacuum lines, glove boxes, and waste-disposal facilities for the safe handling of large amounts of tritium (Evans et al., 1985).

Purification of Maltose-Binding Protein. MBP was purified from periplasmic shock fluid (Willis et al., 1974). A total of 10 L of media (32 g of bacto-tryptone, 20 g of yeast extract, 60 g of Na_2HPO_4 (7·H_2O), 30 g of NaH_2PO_4 (1·H_2O), 10 g of NH_4Cl, 5 g of NaCl, 10 mM $MgSO_4$, 1 mM $CaCl_2$, 0.5 mg of $FeCl_3$, 4 g of maltose, and 100 mg of ampicillin per liter) at 37 °C was innoculated with a culture of *E. coli* PD1(pPD1) containing the gene for MBP on an ampicillin resistance selectable vector (Duplay et al., 1984). After growth to late exponential phase, the cells were chilled and harvested with a Sharples continuous centrifuge and washed once with 30 mM Tris-HCl, pH 7.5, at 4 °C. For the osmotic shock, the cells were resuspended in a 20-fold volume of buffer (i.e., 4 L for 200 g wet weight of cells) of 20% sucrose, 1 mM Na·EDTA, 30 mM Tris-HCl, pH 7.5, at 4 °C, centrifuged (Sorval GS-3 rotor, 6000 rpm, 15 min), and the pellet was homogenized into a liquid paste by stirring. The cell slurry was rapidly dispersed into another 20-fold volume of ice-cold distilled water (with vigorous stirring), and 1 mM $MgCl_2$, 10 mM Tris-HCl, pH 7.5, to 10 mM, and 3 mM NaN_3 were added to achieve the final concentrations shown. Finally, the shock fluid was cleared of cells and debris by two successive centrifugations and filtering through 8-μm and 0.65-μm Millipore filters. DNAse I (~5000 units) and Cellite were added before filtering.

To purify MBP from the crude shock fluid, the shock fluid was passed in several runs through an affinity column (1000-mL bed volume) of cross-linked amylose (Ferenci & Klotz, 1978). MBP (≥99% pure) was eluted from the column by the addition of 10 mM maltose. In this way, up to 1 g of MBP could be purified from 10 L of bacterial culture, sufficient for 5 or 6 NMR samples.

In the course of studies of longer maltodextrins, a contaminating amylase activity was discovered in the MBP preparations, possible due to the *malS* gene product (Freundlieb & Boos, 1986). Subsequent MBP preparations were repurified by passage on a DEAE anion-exchange column. This reduced the amount of amylase activity partially but not completely.

MBP was extensively dialyzed to remove bound maltose, as described by Silhavy et al. (1975). In a typical dialysis, 300 mg of MBP in 300 mL was dialyzed against 10 changes of 18 L of buffer (15 mM K_2HPO_4, 5 mM KH_2PO_4, 3mM NaN_3, pH 7.4) with at least 5 days between changes. After dialysis, MBP was concentrated (~100-fold) by ultrafiltration with a Millipore probe concentrator to approximately 2–3 mM MBP. The concentrated sample was then lyophilized and redissolved in D_2O to give the same concentration of buffer and protein. The concentration of MBP was estimated by optical absorbance of a 200-fold dilution at 280 nm with an extinction coefficient of 1.7 ($\epsilon_{1cm}^{0.1\%}$). This coefficient is slightly lower than that published by Miller et al. (1983) but gave better agreement with dry weight determinations and the stoichiometries observed by NMR spectroscopy.

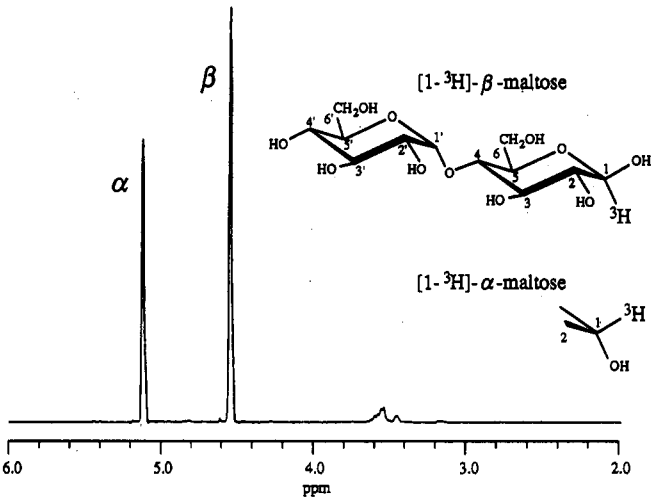

FIGURE 1: Structure and ^{1}H-decoupled tritium spectrum of [1-^{3}H]maltose at 320 MHz. The two resonances at 5.15 and 4.55 ppm are from α-maltose and β-maltose, respectively, present at equilibrium in a 2:3 ratio. The structures of the two anomers of maltose are shown above the spectrum. A number of small resonances (probably from low-level labeling at other sugar positions) are also visible at 3.5–3.6 ppm. Acquisition and processing parameters are described under Materials and Methods.

NMR Spectroscopy of Labeled Samples. NMR spectroscopy of labeled samples was carried out as described previously (Newmark et al., 1990, Williams et al., 1988) on a Bruker AF-300 spectrometer equipped with a tritium channel at 320.13 MHz (7.05 T) and a dual $^1H/^3H$ 10-mm probe. As a precaution against sample spillage, 8-mm Teflon liners with stoppers were used inside 10-mm glass tubes. Aside from routine monitoring of urine tritium levels, no other precautions were required during the acquisition of spectra.

Tritium spectra were referenced to the proton resonance of TMS with a conversion factor of 1.06663974 for obtaining the equivalent tritium frequency (Bloch et al., 1947; Anderson & Novick, 1947; Bloxsidge et al., 1979). Tritium is spin 1/2 so that its line widths are directly comparable to equivalent proton line widths.

The spectrum in Figure 1 was acquired on 200 μL of 50 mM maltose labeled on the anomeric (C1) carbon with 100 mCi of tritium at 25 °C. The spectral width was 3400 Hz with a 3.6-μs (65°) pulse length, 8192 data points, a 4.8-s recycle delay, and 128 scans. Lorentzian-to-Gaussian resolution enhancement (LB = −1, GB = 0.15) and zero-filling to 16K points were applied before Fourier transformation. Composite pulse broad-band proton decoupling (WALTZ-16) was applied to suppress coupling to the neighboring C2 proton. This had the added advantage of adding a nuclear Overhauser effect enhancement. The $J_{^3H-^1H}$ splitting observed in the absence of proton decoupling was 4 Hz for α-G2 and 8 Hz for β-G2, in agreement with the reported $^1H-^1H$ coupling constant (Usui et al., 1974). Spectra taken in the presence of MBP were not

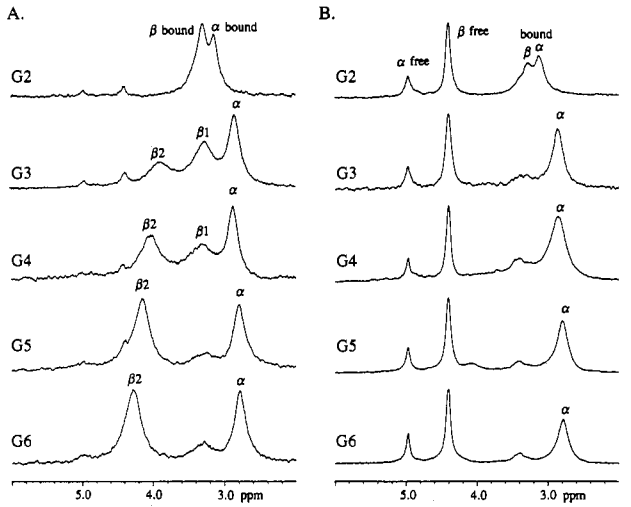

FIGURE 2: Tritium NMR spectra of labeled maltodextrins bound to MBP. [1-^{3}H]Maltodextrins, maltose (G2) through maltohexaose (G6), were freshly added to MBP at below 1:1 (sugar to MBP) stoichiometry (panel A) and between 1.5:1 and 2:1 stoichiometry (panel B). In the low ratio spectra, only bound sugar peaks are present, while in the high ratio spectra both free and bound peaks appear. Bound β peaks are decreased at higher ratios due to the higher affinity of MBP for α-maltodextrins. Bound peak assignments, α, β1, and β2, correspond to binding modes shown in Figure 5. Peaks from other labeled positions in the maltodextrins are visible at 3.5 ppm in several of the spectra, particularly in panel B. Small peaks from labeled glucose are visible at 5.0 and 4.5 ppm in panel A, G2. Acquisition and processing parameters are described under Materials and Methods.

decoupled. Due to the long correlation times of maltose bound to MBP (and exchange broadening of free resonances), splitting due to proton couplings was generally not observed in tritium spectra taken in the presence of MBP.

Titrations of labeled maltodextrins into MBP were preformed at 10 °C to slow the rate of anomeric interconversion. In a typical experiment, an MBP sample was titrated to between 0.5 and 1 stoichiometry (sugar to protein) by the addition of labeled maltodextrin and a spectrum of 1 h acquired (Figure 2A). At this point, either the sample was further titrated to 2:1 stoichiometry and a spectrum acquired (Figure 2B) or a 2-D experiment was run (Figure 4C) and the equilibrium α/β ratio of the sample measured after 2–3 days (Figure 4A,B). One-dimensional spectra were acquired at 10 °C with a 1.2-s recycle delay, a 9-μs (65°) pulse, and a 3400-Hz (10.6 ppm) spectral width with 8192 points. Spectra were averaged for varying times but generally for 1 h (3000 scans) and were processed with 5 Hz of Lorentzian line broadening before Fourier transformation and phasing. Chemical exchange 2-D EXSY spectra were acquired at 10 °C with TPPI phase-sensitive detection and mixing times of 100 ± 25 ms with a 1-s recycle delay. For Figure 3A, NS = 800 scans were averaged per t_1 value, NE = 94 t_1 values were collected, and the spectrum was processed with 5-Hz line broadening in each dimension. For Figure 3B, NS = 352, NE = 128, LB2 = 10 Hz, and LB1 = 5 Hz. For Figure 4C, NS = 2048, NE = 37, and Lorentzian-to-Gaussian apodization was applied with LB2 = LB1 = −10 Hz, GB2 = 0.32, and GB1 = 0.138. All spectra were collected with 1024 points in t_2 and zero-filled to 1024 points in t_1 before Fourier transformation.

Results

^{3}H Spectrum of Maltose. The proton-decoupled tritium spectrum of [1-^{3}H]maltose is shown in Figure 1. Two resonances are present since, like all reducing sugars, maltose exists in solution as a mixture of two anomers, α and β, that differ in the stereochemical configuration of the hydroxyl and hydrogen on the reducing C1 carbon. The assignment of the tritium resonances was based on the assignment of the proton spectrum of maltose (van der Veen, 1963; De Bruyn et al., 1975; Usui et al., 1974). The equilibrium ratio between the two anomeric forms, α- and β-G2, was approximately 2:3. This ratio was the same for all of the maltodextrins examined. In addition, the chemical shifts of all the [1-^{3}H]maltodextrins, including maltose, were the same to within 4 Hz (data not shown). (Small differences in chemical shift are seen due to temperature dependence of the lock solvent resonance.) A number of small resonances are also present at 3.6 ppm. These peaks are most likely due to low-level labeling of other sites in maltose since similar peaks were seen in all of the labeled maltodextrins (data not shown) and occur in a region with appropriate chemical shifts.

In order to estimate the rate of interconversion of the two anomers, the conversion of α-D-glucose to β-D-glucose was studied. From this, we estimate that the time for half-equilibration of maltose and maltodextrin anomers was 3.5 h under our experimental conditions (10 °C, K·PO$_4$ buffer, pH 7.4). In experiments on samples with maltodextrin/MBP ratios of less than 1, more time appeared to be required to reach anomeric equilibrium (on the order of several days). This suggests that the interconversion rates are slowed when the sugars are bound to MBP. The rates of interconversion were not so slow, however, as to imply interconversion of bound sugars necessarily occurred through disassociation of the maltodextrin–MBP complex.

Titration of [1-^{3}H]Maltodextrins into MBP. The tritium NMR spectra of the various maltodextrins in the presence of MBP are shown in Figure 2. Two phases could be distinguished during the titration of maltodextrins into MBP. In the presence of excess binding sites (Figure 2A), essentially all of the labeled molecules were bound, and only the resonances due to maltodextrins bound to MBP were visible. These bound resonances were broad due to the long correlation times of the MBP–maltodextrin complex and were shifted upfield. No free maltodextrin resonances were observed due to the high affinity of MBP.

The second phase of the titrations was reached when the concentration of maltodextrin was increased to beyond 1-to-1 stoichiometry (Figure 2B) and free maltodextrin resonances appeared at their normal chemical shifts (in the absence of MBP). Slow-exchange kinetics were observed between bound and free maltodextrin resonances, but some exchange broadening was present as the free maltodextrin resonances were considereably broader than the free resonances in the absence of protein. In addition, the line widths of the free and bound resonances showed opposite temperature behavior. At higher temperatures, the free sugar resonances broadened while the bound maltodextrin/MBP resonances narrowed (data not shown).

All of the maltodextrin resonances showed an upfield chemical shift change upon binding to MBP. The shift was consistently large for the α anomers (up to 2.2 ppm) but varied between 0.1 and 1 ppm for the β anomers. The large size of the shift suggests that the labeled reducing end of the maltodextrin makes direct contact with an aromatic residue in the protein binding site (Johnson & Bovey, 1958). The line widths of bound β-maltodextrins appear to be slightly larger than those of α-maltodextrins. This is true for G2 (compare the line shapes of the α–α and β–β cross-peaks in Figure 3A) and is clearly the case in the spectra of the longer maltodextrins at low maltose/MBP ratios (Figure 2A). In part, this may

be due to stronger dipolar relaxation of the ^{3}H nucleus when axial (β) versus equatorial (α) but could also arise from chemical-exchange phenomena.

Assignment of Bound Resonances. The assignment of the bound resonances was determined in part by 2-D chemical exchange (EXSY) experiments (Jeener et al., 1979). Two representative experiments, for G2 and G3, are shown in Figure 3. Transfer of magnetization by chemical exchange between bound and free maltodextrins gives rise to the observed cross-peaks. In the 2-D spectrum of maltose (Figure 3A), the cross-peaks identify the upfield bound resonance at 3.15 ppm as bound α-G2 and the downfield resonance at 3.3 ppm as bound β-G2. The extra weak resonances seen in Figure 1 appear as a narrow streak on the diagonal at 3.4 ppm.

In the 2-D EXSY spectrum of G3, only one cross-peak was observed (Figure 3B). This cross-peak identifies the single bound resonance as α-G3. No exchange with free β-G3 resonance was detected because very little β-G3 is bound in the presence of excess α-G3. This can be seen immediately upon comparison of the high and low maltose/MBP ratio spectra of G3 in Figure 2. EXSY experiments with the longer maltodextrins G4–G6 gave essentially identical spectra with that of G3.

Anomeric Specificity. Comparison of the high and low ratio spectra of Figure 2 shows that the ratio of bound α and β peaks changed upon addition of excess maltose. This change represents a difference in affinity of MBP for the two anomeric forms. For maltose (G2), the effect is relatively small and represents roughly a 2-fold change in the ratio of bound α- to bound β-G2. The presence of the peaks from labels at the nonanomeric positions on the shoulder of the bound β peak, and the overlap between the two bound peaks makes more accurate estimation of this ratio difficult. The high ratio spectra of Figure 2B can be used to calculate the ratio of dissociation constants for the two anomeric forms

$$K_D^{\beta}/K_D^{\alpha} = \frac{[\beta]_{free}\cdot[\alpha]_{MBP}}{[\alpha]_{free}\cdot[\beta]_{MBP}} \quad (1)$$

where $[\alpha]_{free}$ and $[\beta]_{free}$ are the concentrations of the free maltodextrin anomers and $[\alpha]_{MBP}$ and $[\beta]_{MBP}$ are the concentrations of the bound forms.

Differences in affinity for α- and β-maltodextrins were also seen in the time dependent behavior of MBP/maltodextrin samples. When low maltose/MBP samples were allowed to reach anomeric equilibrium, the ratio of α to β anomers changed due to the presence of MBP. For G2, this engendered a small change, but for the longer maltodextrins, G3–G7, almost all of the β anomers disappeared (Figure 4A,B). Comparison of the equilibrium α/β ratios in the presence and absence of MBP also allows calculation of the ratio of binding affinities by eq 1. We estimate that the ratio of affinities, K_D^{β}/K_D^{α}, is 2.7 ± 0.5 for maltose (at 10 °C) and is roughly 20 ± 10 for G3 through G6. The large error estimates are due to the difficulty of accurately integrating the very broad bound resonances and the fact that spectra were not acquired under fully relaxed conditions.

Multiple Bound β Conformations. Examination of the low sugar/MBP ratio spectra of G3 and G4 shows two bound β resonances, labeled β1 and β2 in Figure 2A. When the longer maltodextrins G5 and G6 were examined, the β1 resonance had almost completely disappeared and was indistinguishable from the extra peaks at 3.4 ppm. The assignment of the two peaks at β anomers was based on three observations: (1) upon over titration both β peaks disappeared (Figure 2B), (2) upon anomeric equilibration both β1 and β2 peaks decreased concomitant with an increase in the bound α peak (Figure 4A), and (3) the two β resonances were in rapid chemical exchange with each other as shown by saturation transfer experiments

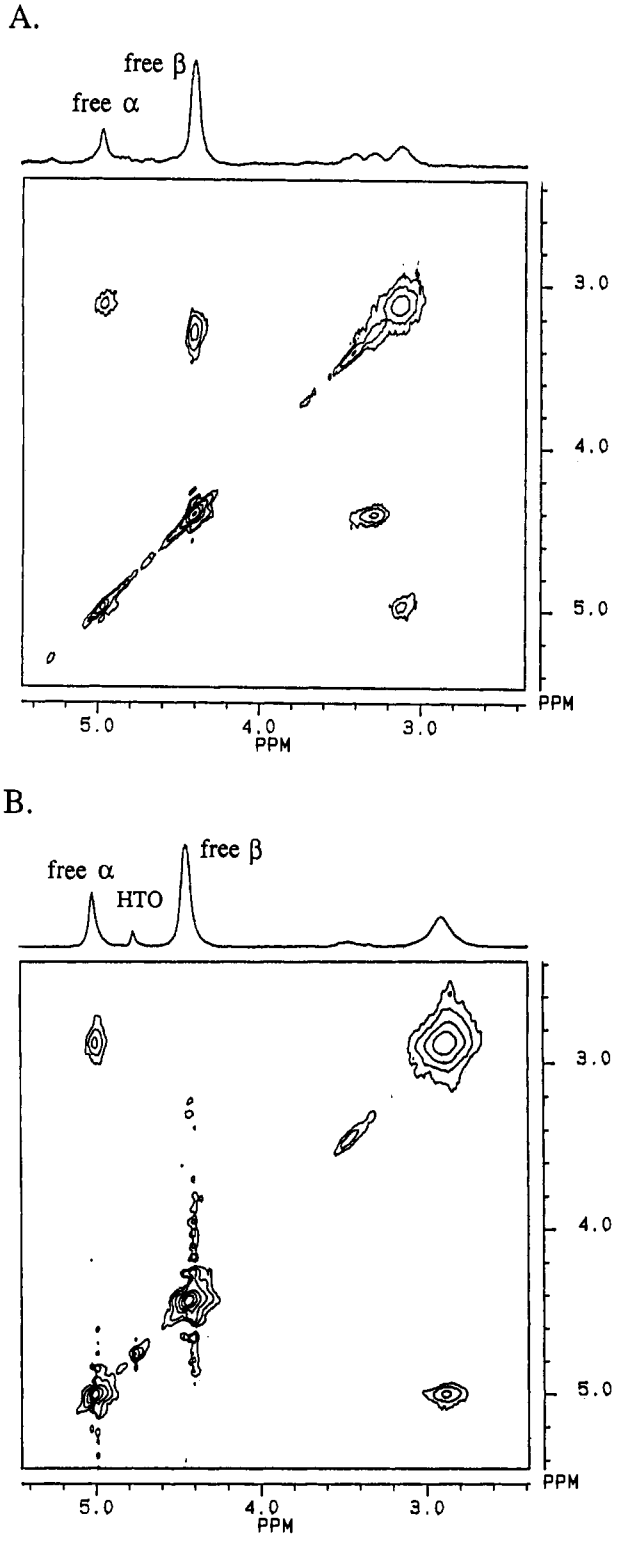

FIGURE 3: 2-D chemical exchange spectra of labeled maltodextrins and MBP. Phase-sensitive exchange (EXSY) spectra were acquired on high sugar/MBP samples with maltose (A) and maltotriose (B). Peaks off the diagonal are due to chemical exchange between the bound and free forms of the maltodextrins and identify the bound peaks as either α or β. The vertical (t_2) projections are shown above each 2-D plot; the free peaks are labeled and the exchange cross-peaks indicate the chemical shifts of the bound resonances. The diagonal resonance at about 3.5 ppm comes from nonanomeric sugar resonances, and HTO is tritiated water. Acquisition and processing parameters are described under Materials and Methods.

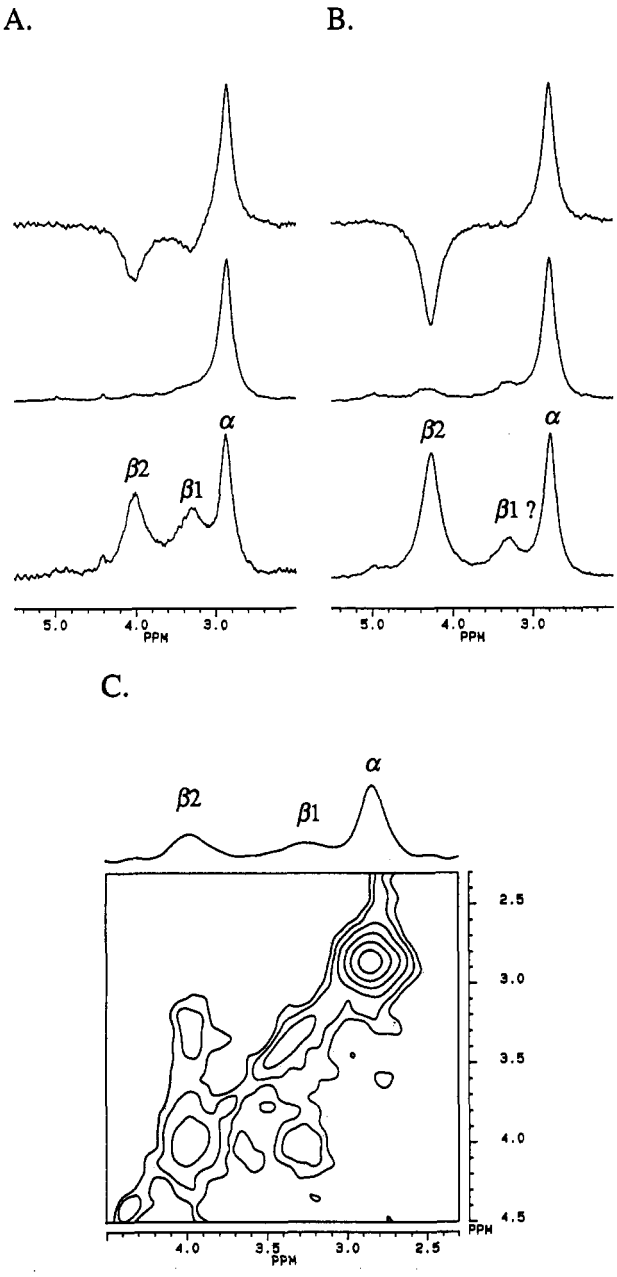

FIGURE 4: Identification of the two bound β peaks by anomeric equilibration and 2-D spectroscopy. (A) Bottom: tritated maltotetrose (G4) immediately after addition to MBP at less than a 1:1 mole ratio. Middle: the same sample after time was allowed for anomeric equilibration (several days). Top: the difference between middle and bottom spectra, demonstrating anomeric interconversion. (B) Bottom: tritiated maltohexose (G6) immediately after addition to MBP at less than a 1:1 mole ratio. Middle: the same sample after time was allowed for anomeric equilibration (several days). Bottom: the difference between middle and bottom spectra, demonstrating anomeric interconversion. Spectra were plotted to a constant height. (C) 2-D EXSY spectrum of low G4/MBP shows that the $\beta 1$ and $\beta 2$ peaks are in rapid chemical exchange with each other. Because of anomeric equilibration before and during the experiment, the bound β peaks are greatly reduced relative to the bound α peak. The first block of the 2-D data set is shown above the 2-D spectrum.

(data not shown) and 2-D EXSY experiments (Figure 4C).

Discussion

Anomeric specificity in MBP was detected in two ways: (1) displacement of one anomer by the other when the ratio of sugar/MBP was >1 and (2) changes in the total amount of each anomer present due to equilibration in the presence of excess MBP. Because the competition for binding between two species can be directly followed, NMR spectroscopy is particularly well suited to measuring small differences in affinity. In the case of maltose, the free-energy difference between the bound α and β forms is only 620 ± 100 cal/mol while the average free energy of binding is 7100 cal/mol (Schwartz et al., 1976). In cases where the two bound anomers are better separated from each other, it should be possible to measure free-energy differences of only 250 cal/mol accurately.

The presence of two bound β resonances for G3 and G4 implies that there are two distinct MBP–sugar complexes. On the basis of the spectra of all the maltodextrins, we believe that these two complexes (or binding modes) are distinguished either by the presence of the reducing end of the maltodextrin in the MBP-binding site ("end-on" binding, $\beta 1$ resonances in Figure 2B) or by MBP binding to the middle glucose residues of the maltodextrin ("middle binding", $\beta 2$ resonances in Figure 2B). This model is illustrated in Figure 5. For linear maltodextrin substrates, both binding conformations are available, and the dominant binding conformation depends on the relative binding affinities. Circular maltodextrins bind in the middle-binding mode since, obviously, no end is available for end-on binding.

The affinity of MBP for G2, G3, longer maltodextrins, and circular maltodextrins has been measured by a mixture of fluorescence spectroscopy (Miller et al., 1983; Szmelcman et al., 1976) and equilibrium-binding techniques (Ferenci et al., 1986; Schwartz et al., 1976; Silhavy et al., 1975). In general, the presence of two different anomers in these studies complicates their interpretation. This is particularly true for the equilibrium-binding studies where the ratio of α to β forms could change during the experiment. It is, however, clear that G3 and longer maltodextrins bind with higher affinity than maltose and that circular maltodextrins (cyclodextrins) bind with an affinity similar to that of maltose. The results of these studies are summarized for three substrates, G2, G3, and G6, in Figure 5. Comparisons between the different sugars are made on the basis of published or estimated binding constants. Within each row, the relative affinity of the different binding modes is calculated on the basis of the tritium NMR spectra, as discussed below.

This model accounts for a large number of features in the spectra. In particular, the presence of an aromatic residue in the MBP-binding site allows us to separate spectroscopically the different binding modes. When bound end-on, the labeled end of the maltodextrin is in close contact with the aromatic residue and the triton label (^{3}H nucleus) experiences a large upfield ring current shift. This is the case for α-maltodextrins and β-maltodextrins in the $\beta 1$ resonance. Evidently, α-maltodextrins are better situated than β-maltodextrins to make this contact, and the closeness of the contact increases with length of the α-maltodextrin. When bound in the middle mode, the triton on the reducing end of β-G3 is moved away from the aromatic residue and experiences a smaller ring current shift, perhaps even from a different residue. As the maltodextrin lengthens, the triton moves further and further from the aromatic residue but continues to experience a small ring current shift because the middle or $\beta 2$ resonance is actually a fast-exchange average of the maltodextrins bound in different "frames" or "registers". This explains the smooth and continual change in chemical shift of the $\beta 2$ resonances with increasing maltodextrin length.

The relative affinities of the two binding modes depend on the length and on the anomeric conformation of the maltodextrin. For α-maltodextrins, end-on binding has a much

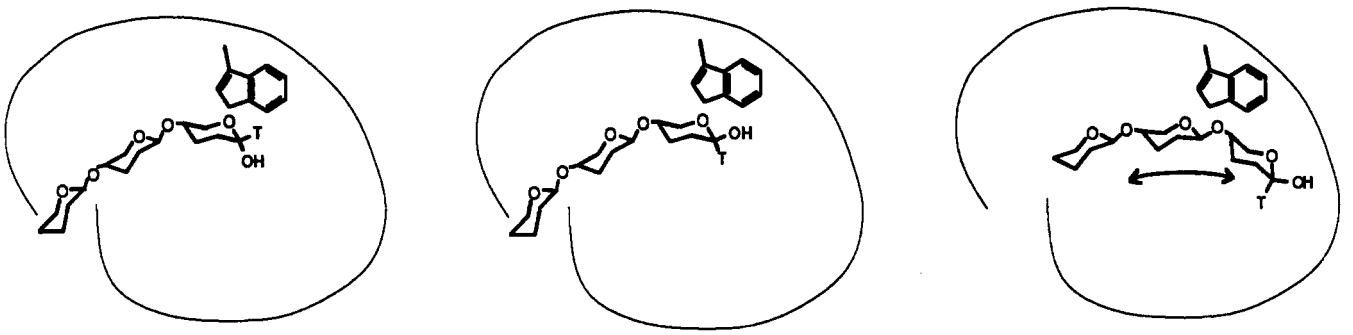

affinity for	α end on	β end on	β middle
G2	med	low	v.low
G3	high	low	low
G6	high	low	med

FIGURE 5: Proposed model for maltodextrin binding to MBP. The two binding modes are shown along with their relative affinities and models. The affinity of a particular binding mode depends on the anomeric conformation and length of the maltodextrin. These are classified as either very low, low, medium, or high. While large uncertainties exist (particularly in comparisons between columns), we estimate that these correspond to relative affinities of <0.2 (v. low), 1 (low), 3 (med), and 15 (high) with errors of up to a factor of 2. The bound peaks in Figure 2 labeled α, β1, and β2 correspond to α end-on, β end-on, and β middle binding, respectively. In the binding models, the six-membered rings represent a linear maltodextrin with either α or β conformation at its reducing end. The surrounding line represents MBP with an aromatic residue in the proximity of the binding site. The α end-on and β end-on binding modes place the reducing end of the maltodextrin in close proximity to the aromatic ring in the MBP-binding site. β middle is an average of several binding conformations (for G4 and longer maltodextrins) where the middle of the maltodextrin oligosaccharide chain occupies the MBP site. As indicated by the arrow, these conformations are in fast exchange on the NMR time scale, and only a single averaged resonance is observed.

higher affinity than middle binding, and, hence, only end-on binding is detectable in the spectra of Figure 2. For β-maltodextrins, the affinity of end-on binding is lower than that for α, comparable to the affinity of middle binding and both modes may be observed. (The affinity of middle binding should be independent of the anomeric conformation and depend only on the length of the maltodextrin.) The principal binding mode, in the case of β-maltodextrins, depends on the length of the maltodextrin. For β-maltose, only end-on binding is observed because the shortness of the molecule precludes middle binding. As the length of the maltodextrin increases, the affinity of middle binding increases. Therefore, for β-maltotriose (G3), we find both binding modes but with roughly twice as much end-on binding as middle binding. For G4, the ratios are almost reversed, and, for G5 and G6, middle binding dominates to the near exclusion of end-on binding. This increase in affinity of middle binding may be in part due to the large size of the maltodextrin binding site and may also be due to the presence of multiple frames that give rise to a larger apparent (or collective) binding affinity for long maltodextrins [see e.g., McGhee and Hippel (1974)].

The preliminary X-ray crystallographic structure of MBP with maltose shows a number of tryptophan residues in the maltodextrin-binding site (Spurlino, 1988). One of these, assigned to tryptophan 232, is placed at the reducing end of the bound maltose molecule in such a way that it makes closest contact with the hydrogen of α-maltose. On the basis of the current assignment of the X-ray structure, we believe that tryptophan 232 is responsible for the large upfield ring current shifts. We note also that one of the assumptions of the binding model is that only one aromatic group is responsible for the upfield chemical shift changes. While this seems reasonable for α-maltodextrins, it maybe less true for the β2 resonances since their chemical shift changes become quite small and a large number of aromatic residues are present in the vicinity of the MBP-binding site.

In may ways, maltodextrin binding to MBP draws parallels to the well-studied example of the binding of β(1–4)-linked *N*-acetylglucosamine (NAG) oligomers to lysozyme (Philips, 1974). In the crystal structure of lysozyme, six binding sites for NAG can be discerned with different affinities for the sugar monomers. Similarly, one can ask what is the size of the maltodextrin-binding site in MBP? Our results would suggest that the MBP-binding site must recognize at least 4+ residues because the chemical shift of the α-maltodextrins continues to increase until α-G5.

As briefly described above, it appears very likely that α-maltodextrins can also bind in the middle or β2 mode; however, because of the much higher affinity of the end-on binding mode for α-maltodextrins, the middle-binding mode should remain only slightly populated until maltodextrins much longer than G6 are studied. The chemical shifts of the α middle-binding mode should show a behavior similar to that of β middle-binding mode and approach the chemical shift of free α-maltodextrin as the maltodextrin chain length increases. The observation of such a resonance would be strong confirmation of the present binding model. Further studies may also explain the anomalous temperature behavior of the β1 and β2 resonances. Over the limited temperature range studied (5–15 °C), β1 appears to broaden with decreasing temperature and β2 appears to narrow (data not shown). If β2 is, in fact, a summation of resonances in fast exchange, then it should broaden (or not change) with decreasing temperature (McConnell, 1958). In addition, we note that decreasing temperature increases the viscosity of the sample and generally broadens the bound sugar resonances. Because of the relatively rapid anomerization of maltodextrins at higher temperatures, further experiments will require the use of methyl-β-maltodextrins.

Lastly, further studies may also explain the differences between α-G3 and β-G3 end-on binding (Figure 2). The addition of a third glucose residue to α-G2 increases the affinity of binding and causes a further upfield chemical shift (of 0.3 ppm). The same addition to β-G2, however, does not seem to increase the affinity, and there is no chemical shift change in the β1 end-on resonance.

It is worth considering if alternative spectroscopic techniques could have been employed in the present study. Of the two

chemically compatible isotopes, both ^2H and ^{13}C suffer from a lack of sensitivity. For indirect (^1H) detection of ^{13}C-labeled maltodextrins, the large line widths of the proton signal indicate that the ^{13}C-to-^1H transfer would not be very efficient. Deuterium spectroscopy is even less sensitive and suffers the additional problem that the line widths of bound [^2H]maltodextrins would be very broad (up to 7 ppm at 7 T) due to the long correlation times and efficient quadrupolar relaxation of ^2H.

Two types of ^{13}C spectroscopy are possible: carbon-edited proton (inverse detection) and direct detect (with possible magnetization transfer from proton). Although indirect detection is more sensitive, the greater chemical shift dispersion of ^{13}C makes direct detection more attractive. The anomeric α and β resonances of maltose are better separated by ^{13}C spectroscopy than by ^3H (or ^1H) spectroscopy, and one could hope for a similar improvement in resolution of the bound resonances. Unfortunately, aside from sensitivity considerations, the use of ^{13}C-labeled substrates suffers from two additional problems: increased difficulty of synthesis and the presence of background label. One of the advantages of ^3H labeling in the present study was the relative ease and rapidity, given the proper facilities, with which the different substrates could be labeled. The presence of background label (1% natural abundance) in other sites in the substrate and in the macromolecule (MBP) is also a problem with ^{13}C spectroscopy. The background signal from within the substrate itself would range from 11% for maltose to 35% for maltohexaose. In principle, these could be eliminated by the use of ^{13}C-depleted starting materials for the synthesis of the [1-^{13}C]maltodextrins. From MBP, the total background signal can be estimated to be 10 times the selective ^{13}C signal (at 1:1 stoichiometry). This protein signal, however, is broad and has empty windows, notably around 93–97 ppm where the anomeric ^{13}C resonances of free maltodextrins occur (Heyraud et al., 1979; Morris & Hall, 1982). Subtraction techniques could hope to remove most of the MBP background but at a cost of increased experimental complexity and acquisition time.

In comparison, we should compare possible improvements available with ^3H labeling and spectroscopy. Two important limitations of the current study have been the relatively weak signal and the rapid interconversion of sugar anomers. Both of these problems could be solved by the use of tritiated methylmaltodextrin derivatives. Advances in the synthesis of tritiomethyl iodide (Saljoughian et al., 1990) should lead to easy synthesis of 1-*O*-[^3H]methylmaltodextrins with specific activities 10 times higher than those of maltodextrins labeled by the present exchange reaction. With the concomitant increase in signal and possible separation of the two α and β methylmaltodextrin anomers we can hope for elucidation of even more details of maltodextrin binding to MBP. Studies using ^1H–^3H NOEs should also then be feasible and should help clarify the details of the binding modes.

Added in Proof

A more detailed description of the MBP crystal structure has just appeared (Spurlino et al., 1991). On the basis of this refined structure, the residue most likely for the upfield shift of the anomeric ^3H resonance is Trp 230, rather than Trp 232. The large number of other aromatic groups in the binding site confirms that there may be other contributions to the shifts for the β-anomer and "middle" binding modes.

References

Adams, M. D., & Oxender, D. L. (1989) *J. Biol. Chem. 264*, 15739–15742.

Anderson, H. L., & Novick, A. (1947) *Phys. Rev. 71*, 372–373.

Bloch, F., Graves, A. D., Packard, M., & Spence, R. W. (1947) *Phys. Rev. 72*, 551.

Bloxsidge, J. P., Elvidge, J. A., Jones, J. R., Mane, R. B., & Saljoughian, M. (1979) *Org. Magn. Reson. 12*, 574–578.

Chauvet-Monges, A.-M., Monti, J. P., Crevat, A., Gaudin, C., Sari, J.-C., & Belaich, J.-P. (1979) *J. Chim. Phys. Phys.-Chim. Biol. 76*, 714–719.

Clark, A. F., Gerken, T. A., & Hogg, R. W. (1982) *Biochemistry 21*, 2227–2233.

De Bruyn, A., Anteunix, M., & Verhegge, G. (1975) *Bull. Soc. Chim. Belg. 84*, 721–734.

Duplay, P., Bedouelle, H., Fowler, A., Zabin, I., Saurin, W., & Hofnung, M. (1984) *J. Biol. Chem. 259*, 10606–10613.

Evans, E. A., Sheppard, H. C., Turner, J. C., & Warrell, D. C. (1974) *J. Labelled Compd. 10*, 569–587.

Evans, E. A., Warrell, D. C., Elvidge, J. A., & Jones, J. R. (1985) in *Handbook of Tritium NMR Spectroscopy and Applications*, Wiley, Chichester.

Ferenci, T., & Klotz, U. (1978) *FEBS Lett. 94*, 213–217.

Ferenci, T., Muir, M., Lee, K. S., & Maris, D. (1986) *Biochim. Biophys. Acta 860*, 44–50.

Freundlieb, S., & Boos, W. (1986) *J. Biol. Chem. 261*, 2946–2953.

Greenwood, C. T. (1970) in *The Carbohydrates: Chemistry and Biochemistry* (Pigman, W., Horton, D., & Herp, A., Eds.) pp 471–513, Academic Press, New York.

Heyraud, A., Rinaudo, M., & Vignon, M. (1979) *Biopolymers 18*, 167–185.

Hodge, J. E., Rendleman, J. A., & Nelson, E. C. (1972) *Cereal Sci. Today 17*, 180–188.

Jeener, J., Meier, B. H., Bachmann, P., & Ernst, R. R. (1970) *J. Chem. Phys. 71*, 4546–4553.

Johnson, C. E., Jr., & Bovey, F. A. (1958) *J. Chem. Phys. 29*, 1012–1014.

Kellerman, O., & Ferenci, T. (1982) *Methods Enzymol. 90*, 459–463.

Mao, B., Pear, M. R., McCammon, J. A., & Quiocho, F. A. (1982) *J. Biol. Chem. 257*, 1131–1133.

McConnell, H. M. (1958) *J. Chem. Phys. 28*, 430–431.

McGhee, J. D., & von Hippel, P. H. (1974) *J. Mol. Biol. 86*, 469–489.

Miller, D., Olson, J., Pflugrath, J., & Quiocho, F. A. (1983) *J. Biol. Chem. 258*, 13665–13672.

Morris, G. A., & Hall, L. D. (1982) *Can. J. Chem. 60*, 2431–2441.

Newcomer, M. E., Lewis, B. A., & Quiocho, F. A. (1981) *J. Biol. Chem. 256*, 13218–13222.

Newmark, R. D., Un, S., Williams, P. G., Carson, P. J., Morimoto, H., & Klein, M. P. (1990) *Proc. Natl. Acad. Sci. U.S.A. 87*, 583–587.

Philips, D. C. (1974) in *Lysozyme* (Osserman, E. F., Canfield, R. E., & Beychok, S., Eds.) pp 9–30, Academic Press, New York.

Post, J. F. M., Cottam, P. F., Simplaceanu, V., & Ho., C. (1984) *J. Mol. Biol. 179*, 729–743.

Raftery, M. A., Dahlquist, F. W., Chan, S. I., & Parsons, S. M. (1968) *J. Biol. Chem. 243*, 4175–4180.

Quiocho, F. A. (1986) *Annu. Rev. Biochem. 55*, 287–315.

Quiocho, F. A., & Vyas, N. K. (1984) *Nature 310*, 381–386.

Saljoughian, M., Morimoto, H., & Williams, P. G. (1990) *J. Chem. Soc., Perkin Trans. 1*, 1803–1808.

Schwartz, M. (1987) in *Escherichia coli and Salmonella typhimurium: Cellular and Molecular Biology* (Neidhardt,

F. C., Ingraham, J. L., Low, K. B., Magasanik, B., Schaecter, M., & Umbarger, H. E., Eds.) Vol. 2, pp 1482-1502, American Society for Microbiology, Washington, D.C.
Schwartz, M., Kellermann, O., Szmelcman, S., & Hazelbauer, G. L. (1976) *Eur. J. Biochem. 71*, 167-170.
Shen, Q., Simplaceanu, V., Cottam, P. F., & Ho, C. (1989a) *J. Mol. Biol. 210*, 849-857.
Shen, Q., Simplaceanu, V., Cottam, P. F., Wu, J.-L., Hong, J.-S., & Ho, C. (1989b) *J. Mol. Biol. 210*, 859-867.
Silhavy, T. J., Szmelcman, S., Boos, W., & Schwartz, M. (1975) *Proc. Natl. Acad. Sci. U.S.A. 72*, 2120-2124.
Spurlino, J. C. (1988) Ph.D. Thesis, Rice University.
Spurlino, J. C., Lu, G.-Y., & Quiocho, F. A. (1991) *J. Biol. Chem. 266*, 5202-5219.
Sykes, B. D. (1969) *Biochemistry 8*, 1110-1116.
Szmelcman, S., Schwartz, M., Silhavy, T. J., & Boos, W. (1976) *Eur. J. Biochem. 65*, 13-19.
Takusagawa, F., & Jacobson, R. A. (1978) *Acta Crystallogr. B34*, 213-218.
Thomas, E. W. (1966) *Biochem. Biophys. Res. Commun. 24*, 611-615.
Trakhanov, S. D., Chirgadze, N. Y., & Yusifov, E. F. (1989) *J. Mol. Biol. 270*, 847-849.
Usui, T., Yokoyama, M., Yamaoka, N., Matsuda, K., Tuzimura, K., Sugiyama, H., & Seto, S. (1974) *Carbohydr. Res. 33*, 105-116.
van der Veen, J. (1963) *J. Org. Chem. 28*, 564-566.
Williams, P. G., Morimoto, H., & Wemmer, D. E. (1988) *J. Am. Chem. Soc. 110*, 8038-8044.
Williams, P., Morimoto, H., Gehring, K. B., Nikaido, H., Carson, P., Un, S., Klein, M., & Wemmer, D. E. (1989) in *Synthesis and Applications of Isotopically Labelled Compounds 1988 (Proceedings of the 3rd International Symposium, Innsbruck)* (Baillie, T. A., & Jones, J. R., Eds.) pp 487-492, Elsevier, Amsterdam.
Willis, R. C., Morris, R. G., Cirakoglo, C., Schellenberg, G. D., Gerber, N. H., & Furlong, C. E. (1974) *Arch. Biochem. Biophys. 161*, 64-75.
Zukin, R. S. (1979) *Biochemistry 18*, 2139-2145.

Importance of Hydrogen-Bonding Interactions Involving the Side Chain of Asp158 in the Catalytic Mechanism of Papain†

Robert Ménard,‡ Henry E. Khouri,‡ Céline Plouffe,‡ Pierre Laflamme,‡ Robert Dupras,‡ Thierry Vernet,§ Daniel C. Tessier,§ David Y. Thomas,§ and Andrew C. Storer*,‡

Protein Engineering and Genetic Engineering Sections, Biotechnology Research Institute, National Research Council of Canada, 6100 Avenue Royalmount, Montréal, Québec H4P 2R2, Canada

Received January 15, 1991; Revised Manuscript Received March 15, 1991

ABSTRACT: In a previous study, it was shown that replacing Asp158 in papain by Asn had little effect on activity and that the negatively charged carboxylate of Asp158 does not significantly stabilize the active site thiolate–imidazolium ion pair of papain (Ménard et al., 1990). In this paper, we report the kinetic characterization of three more mutants at this position: Asp158Gly, Asp158Ala, and Asp158Glu. From the pH–activity profiles of these and other mutants of papain, it has been possible to develop a model that enables us to dissect out the contribution of the various mutations toward (i) intrinsic activity, (ii) ion pair stability, and (iii) the electrostatic potential at the active site. Results obtained with mutants that place either Gly or Ala at position 158 indicate that the hydrogen bonds involving the side chain of Asp158 in wild-type papain are indirectly important for enzyme activity. When CBZ-Phe-Arg-MCA is used as a substrate, the $(k_{cat}/K_M)_{obs}$ values at pH 6.5 are 3650 and 494 M^{-1} s^{-1} for Asp158Gly and Asp158Ala, respectively, as compared to 119 000 M^{-1} s^{-1} for papain. Results with the Asp158Glu mutant suggest that the side chain of Glu moves closer to the active site and cannot form hydrogen bonds similar to those involving Asp158 in papain. From the four mutations introduced at position 158 in papain, we can conclude that it is not the charge but the hydrogen-bonding interactions involving the side chain of Asp158 that contribute the most to the stabilization of the thiolate–imidazolium ion pair in papain. However, the charge and the hydrogen bonds of Asp158 both contribute to the intrinsic activity of the enzyme.

An understanding of the mode of action of cysteine proteases is of interest for many reasons. Cysteine proteases are members of a class of enzymes that are widely distributed among living organisms and participate in a number of physiological processes in plants, bacteria, and animals (Brocklehurst et al., 1987; Baker & Drenth, 1987). There is a great deal of evidence that implicates cysteine proteases in various disease states. In particular, lysosomal cathepsins are believed to be involved in several pathological conditions such as muscular dystrophy, heart diseases, inflammatory diseases, and tumor invasiveness (Kar & Pearson, 1977; Poole et al., 1978, 1980; Mort et al., 1984; Sloane & Honn, 1984; Rich, 1986). These enzymes form a family of homologous proteins with comparable structures (Kamphuis et al., 1985) and functions, and the information obtained from a given enzyme can be very useful in understanding the behavior of related cysteine proteases. The most widely studied member of this group is the plant protease papain, and it is taken as the prototypic member of this class of enzymes.

The structure of papain has been solved at 1.65-Å resolution and is available (Kamphuis et al., 1984), and the general

† NRCC Publication No. 32763.
* Author to whom correspondence should be addressed.
‡ Protein Engineering Section.
§ Genetic Engineering Section.

0006-2960/91/0430-5531$02.50/0